

# Global PDF-based non-local means filtering of resting fMRI data

Jian Li<sup>1</sup>, Soyoung Choi<sup>1,2</sup>, Richard M. Leahy<sup>1</sup>

<sup>1</sup> Signal and Image Processing Institute, University of Southern California, Los Angeles, CA, USA

<sup>2</sup> Neuroscience Program, University of Southern California, Los Angeles, CA, USA

## Introduction

Identification of brain networks from the temporal and spatial correlation patterns in resting fMRI (rfMRI) data is challenging due to relatively small BOLD signal contrast and poor SNR<sup>1</sup>. 3D Gaussian filtering or 2D Laplace-Betrami (LB) cortical surface filtering is commonly used to reduce noise. Unfortunately, this smoothing also mixes signals from spatially-adjacent functional regions. This in turn confounds delineation of the spatial boundaries of the regions that make up each network. Temporal non-local means (tNLM) filtering resolves this issue using a non-local smoothing kernel<sup>2</sup>, where the kernel weights are determined by a similarity measure between time series. In this way tNLM avoids blurring of functional boundaries while reducing noise through weighted averaging of data with similar temporal behavior. Here we describe tNLM-pdf, an extension of tNLM, that replaces a heuristically chosen filter kernel function with one based on an estimated probability density function representing connectivity between voxels.

## Methods

Surface-based tNLM-pdf filtering adopts tNLM's approach of filtering as a weighted average of signals, where the weights are based on temporal similarities between the rfMRI time series at the vertex being filtered and each of the other vertices in the surface tessellation. This avoids mixing signals across functional boundaries because the time series between distinct functional regions are less correlated than within each region. tNLM-pdf differs from tNLM in two aspects: i) The weighting kernel function  $w(i, j) = 1 - \exp\{-P_s(r)/P_n(r)/h\}$ , where  $r$  is the correlation between time series at vertex  $i$  and  $j$ , and  $P_s(r)$  and  $P_n(r)$  are the estimated PDFs of the Pearson correlation for within-network and between-network vertex pairs, respectively. The PDFs are estimated using a Gaussian mixture model. The parameter  $h$  controls the degree of smoothing and is chosen to maximally separate contributions from within and between networks; ii) for each vertex, we compute  $w(i, j)$  for the entire cerebral cortex, rather than using a restricted neighborhood as in tNLM<sup>2</sup>. After filtering, a normalized graph-cut (N-cuts) algorithm<sup>3</sup> was then used to parcellate the filtered data sets into a set of 10 networks.

## Results

Fig. 1 shows a comparison of unfiltered, LB, tNLM and tNLM-pdf filtered rfMRI data at two different time points for a single subject from the HCP dataset. Unfiltered data show the most spatial detail but also the largest amount of noise, while LB results show low noise characteristics but limited spatial complexity. tNLM and tNLM-pdf fall both between these extremes and exhibit the boundary-preserving properties that characterize NLM filtering. In comparing the two, it appears that tNLM-pdf has more spatial complexity that may indicate an improved ability to identify a more complete set of networks relative to the other processing methods. To explore this further, in Fig. 2 we show an example of parcellation into 10 networks, selecting for display only the 4 sub-networks that delineate the default mode network (DMN). With LB and tNLM filtering, the purple and brown sub-networks are mostly homologous to one another, each constrained to one hemisphere. On the other hand, tNLM-pdf filtered data sub-delineates these larger regions into sub-networks which symmetrically possess regions from both hemispheres indicating

interhemispheric functional correlation. Interestingly, the sub-delineations found by tNLM-pdf filtering in (d) are well aligned with those found in <sup>4</sup> (Fig.2e), which were based on parcellation of 40 subjects.

## Conclusion

tNLM-pdf filtering not only allows us to denoise rfMRI data while preserving spatial structure, but also reveals connections between distal but functionally synchronized regions. Moreover, cortical parcellation based on the tNLM-pdf filtered rfMRI data may allow identification and study of functional sub-divisions of known networks within individuals.

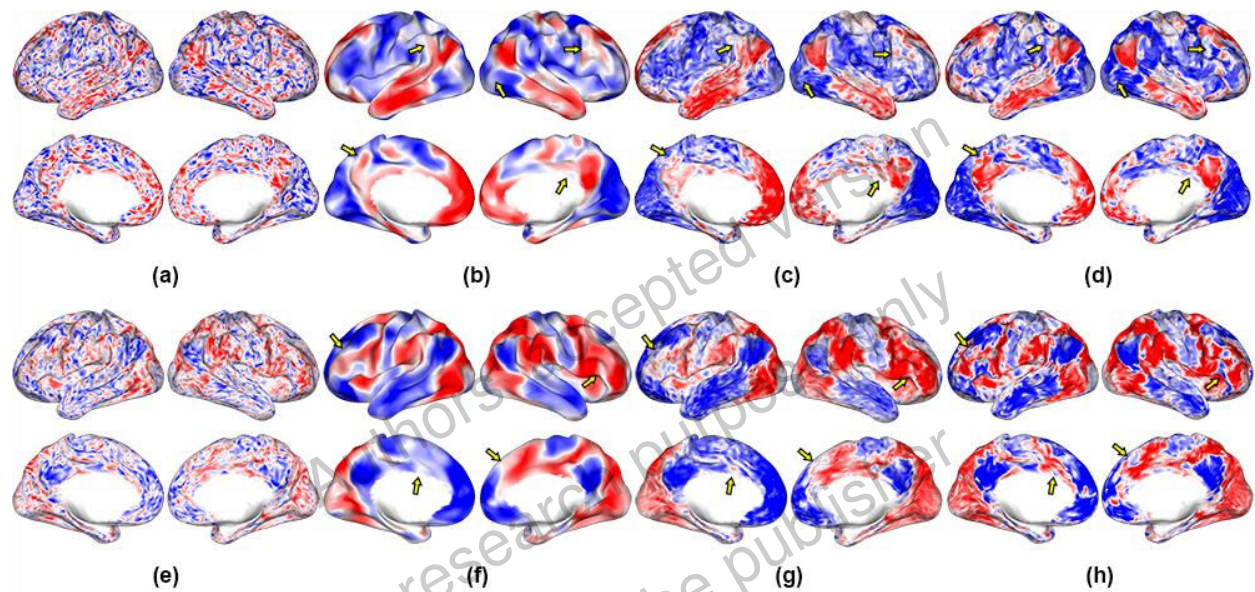


Figure 1: Illustration of the filtering effects on rfMRI data in a single subject at two different time points: 2'20'' for (a) – (d) and 2'54'' for (e) – (h). (a)(e) unfiltered data (b)(f) Gaussian (LB) filtering ( $s=4$ ) (c)(g) tNLM filtering ( $h=0.72$ ) (d)(h) tNLM-pdf filtering ( $h=21.56$ ). Color map ranges from -2 to 2 showing positive (red), negative (blue) and zero (white) BOLD signal strength. All the three filtering results exhibit spatial correlation patterns with differing characteristics. The tNLM-pdf filtered data appears to retain more spatial structure than the LB and tNLM filtered data. The yellow arrows indicate a few interesting ROIs where we can clearly observe these differences.

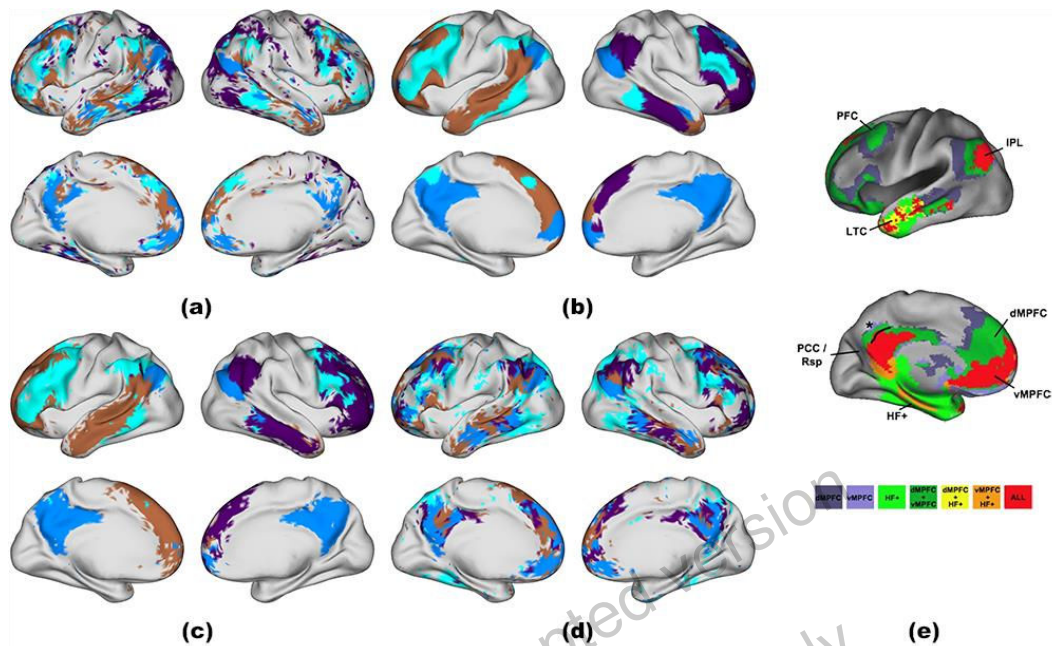


Figure 2: Cortical parcellations using N-cuts into 10 networks for a single subject. Only the four sub-networks that collectively constitute the default mode network (DMN) are shown. (a) unfiltered data (b) Gaussian (LB) filtering ( $s=4$ ) (c) tNLM filtering ( $h=0.72$ ) (d) tNLM-pdf filtering ( $h=21.56$ ) and (e) Figure adapted from [5] that shows sub-delineation of DMN. Each distinct color represents one of the 4 clusters. In LB and tNLM, the brown and dark purple sub-networks do not cross hemispheres while in tNLM-pdf the four sub-networks synchronize well across the two hemispheres and appear to be largely symmetric. The parcellation result using tNLM-pdf filtered data in (d) shows a sub-delineation of DMN, well aligned with the literature as shown in (e), adapted from [5].

## References

1. S. M. Smith, et al., "Correspondence of the brain's functional architecture during activation and rest", *Proceedings of the National Academy of Sciences*, vol. 106, no. 31, pp. 13040–13045, 2009. DOI: 10.1073/pnas.0905267106.
2. C. Bhushan, M. Chong, S. Choi, A. A. Joshi, J. P. Haldar, H. Damasio, R. M. Leahy, "Temporal non-local means filtering reveals real-time whole-brain cortical interactions in resting fMRI", *PLoS ONE*, vol. 11, no. 7, p. e0158504, 2016. DOI: 10.1371/journal.pone.0158504.
3. Jianbo Shi, J. Malik, "Normalized cuts and image segmentation", *IEEE Trans. Pattern Anal. Machine Intell.*, vol. 22, no. 8, pp. 888–905, 2000. DOI: 10.1109/34.868688.
4. R. L. Buckner, J. R. Andrews-Hanna, D. L. Schacter, "The brain's default network: Anatomy, function, and relevance to disease", *Annals of the New York Academy of Sciences*, vol. 1124, no. 1, pp. 1–38, 2008. DOI: 10.1196/annals.1440.011.